

Sensor and Simulation Notes

Note 499

April 2005

**The Relationship Between Feed Arm Position and Input Impedance  
in Reflector Impulse Radiating Antennas**

Everett G. Farr and Leland H. Bowen  
Farr Research, Inc.

**Abstract:**

For many years reflector Impulse Radiating Antennas (IRAs) were built with four feed arms positioned at  $\pm 45^\circ$  to the dominant polarization (usually vertical). However, recent experimental and numerical investigations have demonstrated improved gain and crosspol performance when the feed arms were positioned at  $\pm 30^\circ$  to vertical. Despite these results, there has been a belief that one could obtain a better TDR and lower return loss with feed arms positioned at  $\pm 45^\circ$ . Because a flat TDR is especially desirable in radar applications, designs with feed arms at  $\pm 30^\circ$  have been slow to be accepted. We compile here TDR data on several pairs of IRAs that are similar except for their feed arm positions. In controlled comparisons, we find no appreciable advantage in the TDRs of IRAs with feed arms positioned at  $\pm 45^\circ$ . This suggests that the  $\pm 30^\circ$  configuration is preferred because of its other advantages.

## I. Introduction

We consider here the optimal position of feed arms in reflector Impulse Radiating Antennas (IRAs). In the early years, IRAs had four evenly distributed feed arms positioned at  $\pm 45^\circ$  to vertical (for vertical polarization). This configuration was used primarily because it simplified the calculation of the input impedance. Later, we demonstrated a variety of improvements to the IRA by positioning the feed arms at  $\pm 30^\circ$  to vertical [1, 2]. These improvements included increased gain, decreased crosspol gain, and a more equal beamwidth in the two principal planes. These results were consistent with the earlier numerical work of Tyo [3].

Despite the proven advantages of positioning the feed arms at  $\pm 30^\circ$ , much doubt has remained about the newfangled design. It is widely believed that a design with feed arms at  $\pm 45^\circ$  has a flatter TDR and a lower return loss. These features are especially critical in UWB radar systems, where spurious reflections may contaminate the data.

The belief that IRAs with feed arms at  $\pm 45^\circ$  have superior TDRs is based on early data showing very flat TDRs of such devices [4, 5]. However, those papers did not offer a one-to-one comparison between similar IRAs with feed arms in both positions. We attempt to fill in some of those gaps here.

We begin this paper by reviewing the case for positioning the feed arms at  $\pm 45^\circ$ . We do so by reviewing some of the TDR data on large IRAs built by Giri *et al.* We then review the case for  $\pm 30^\circ$  by reviewing gain and crosspol data on our two best 46-cm IRAs with feed arms at both  $\pm 30^\circ$  and  $\pm 45^\circ$ . We then examine the TDRs of four pairs of similar IRAs with feed arms at both positions. We do so in order to determine if designs with arms at  $\pm 45^\circ$  really exhibit an improved input impedance match over designs with arms at  $\pm 30^\circ$ . Finally, we offer our analysis of the advantages of the two designs and recommendations for further work.

## II. The Case for $\pm 45^\circ$ : Smooth TDR In Large IRAs Without Baluns

We begin by reviewing the case for positioning feed arms at  $\pm 45^\circ$ . We make that case by showing TDR data from Reference [5] that demonstrates that large IRAs with feed arms positioned at  $\pm 45^\circ$  can have very smooth TDRs. Similar data is available in [4]. We reproduce the data from [5] (with permission of the authors) to make the comparisons to later designs clear.

In Figure 2.1, we see the test assembly for measuring the TDR of a 1.83-meter (6-ft) reflector IRA. Note that there is no balun in this configuration. A single cable is run along one of the feed arms that attaches across the gap at the focus as a 50-to-200  $\Omega$  discontinuity.

In Figure 2.2, we see a photo of the IRA with the TDR cable attached. Note that the cable is run along a path that avoids the resistors, which may make the resistors more effective in smoothly terminating the feed arms. We explore the importance of this in Section V of this paper. Finally, in Figure 2.3 we see the raw TDR data. We note that the TDR is quite smooth, which indicates a good impedance match at the end of the feed arms.

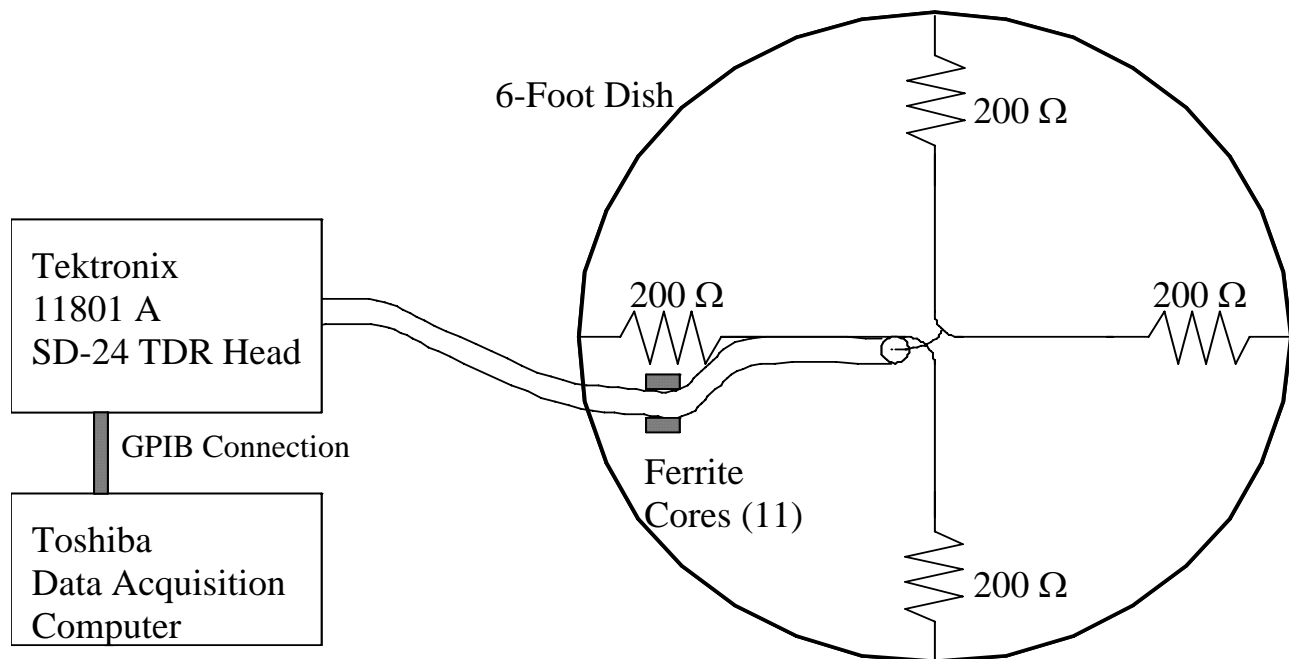


Figure 2.1. Schematic Diagram of Test Assembly (Figure 1 in [5]).

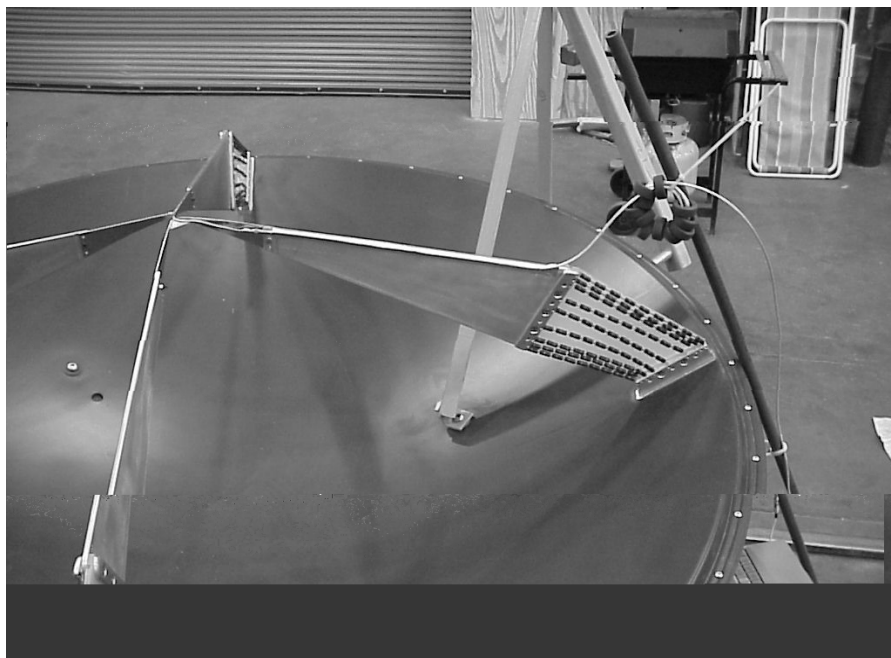


Figure 2.2. TDR Test Assembly (Figure 2 in [5]).

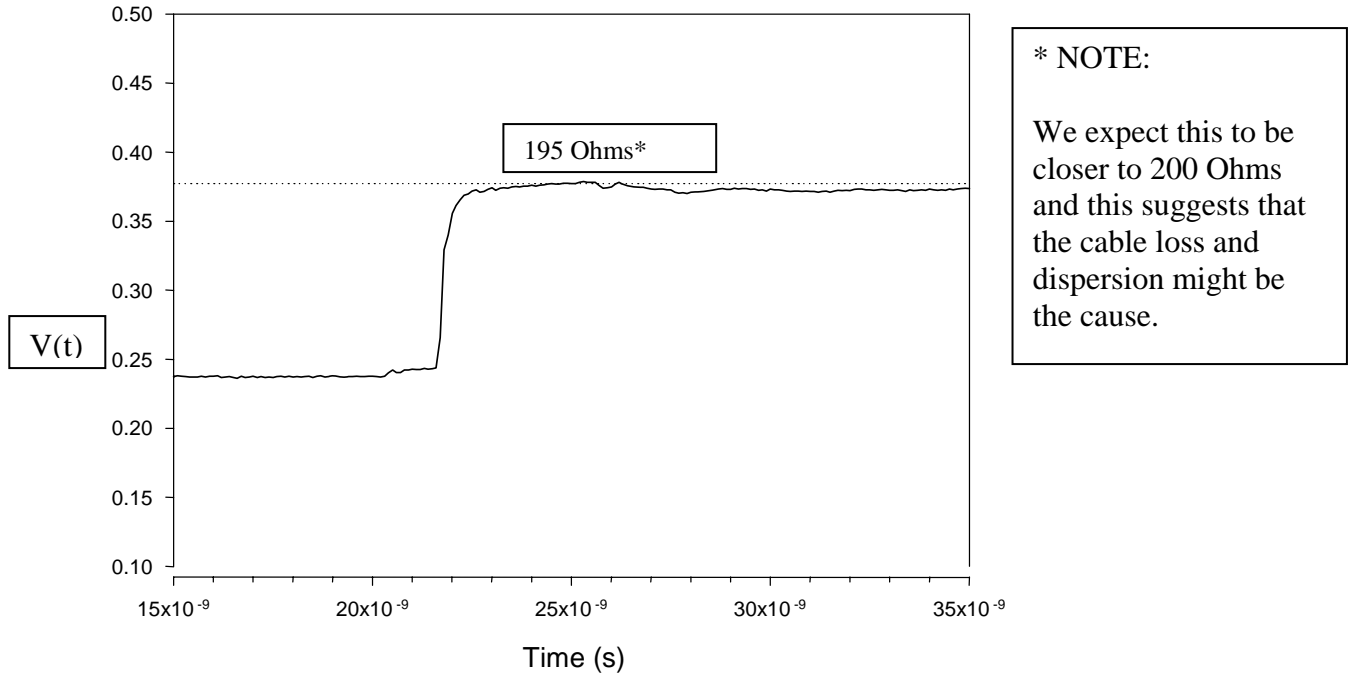


Figure 2.3. TDR Data for the 6-Foot IRA acquired with a 200 Ohm termination (Figure 6 in [5])

Because the TDR of Figure 2.3 is so smooth, this data has been used to infer that all designs with feed arms positioned at  $\pm 45^\circ$  have better (flatter) TDRs than similar designs could have with feed arms positioned at  $\pm 30^\circ$ . This is inferred by comparing the TDR of a large antenna (1.8 m, 6 ft.) with carbon-composition resistors and feed arms at  $\pm 45^\circ$  to a smaller antenna (46 cm, 18 in.) with metal film resistors and feed arms at  $\pm 30^\circ$ . However, no one-to-one comparison of two large antennas with feed arms at both positions has ever been made. In Section IV, we do the comparison for a variety of similar IRAs.

### III. The Case for $\pm 30^\circ$ : Gain and Crosspol Comparison

The improvements available in the  $\pm 30^\circ$  designs are documented exhaustively elsewhere [1-3], but it may be useful to review the most important difference. We overlay the realized copol and crosspol realized gains of the IRA-1B ( $\pm 45^\circ$ , distributed resistors) and IRA-3 ( $\pm 30^\circ$ , resistors at edge of feed arms) in Figure 3.1. We will see later that these are our two best examples of design for their respective feed arm positions with a diameter of 46 cm (18 in.). The IRA-1B is shown later in Figure 4.9, and the IRA-3 is shown later in Figures 4.13 and 4.14. We observe in Figure 3.1 that the realized gain of the IRA-3 is somewhat better than that of the IRA-1B. The crosspol rejection, however, is substantially improved in the IRA-3 over the IRA-1B. These results for gain are consistent with the earlier numerical results of Tyo in [3]. This makes the case in favor of using feed arms at  $\pm 30^\circ$ .

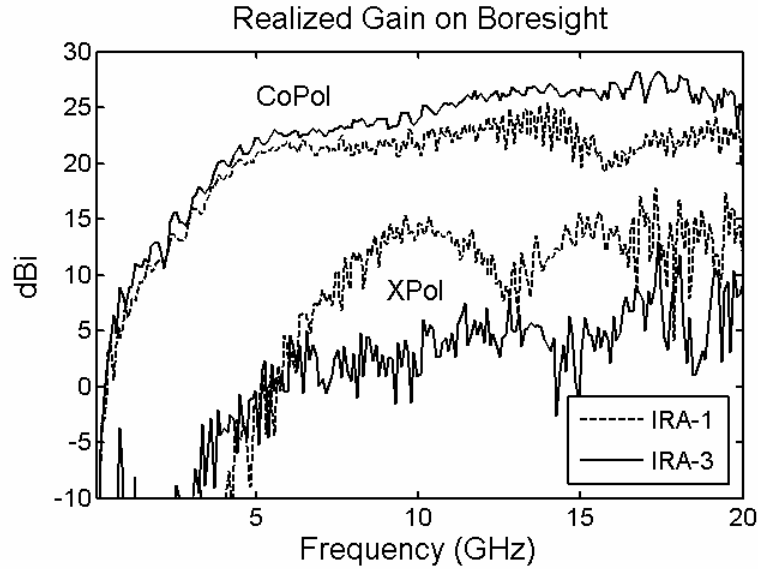


Figure 3.1. Realized gain for IRA-1 & IRA-3

#### IV. Comparisons

We begin now our comparison of the TDRs of similar IRAs that differ only in the position of their feed arms.

Our first comparison consists of early versions of the IRA-1 and IRA-2, as shown in Figures 4.1 and 4.2. These antennas have a spun aluminum parabolic reflector that is 46 cm (18") in diameter with a focal length of 23 cm ( $F/D = 0.5$ ). The IRA-1 has feed arms positioned at  $\pm 45^\circ$  to vertical and the IRA-2 has feed arms positioned at  $\pm 30^\circ$  to vertical [1]. The load resistors used on these two antennas are high voltage, non-inductive, carbon composition resistors from HVR Advanced Power Components, Inc. There are two 400- $\Omega$  resistors in parallel at the end of each arm.

The TDRs of the IRA-1 and IRA-2 are shown in Figures 4.3 and 4.4. Note the large dip in the impedance at the load resistors, even though the values of the resistors match the impedance of the feed arms. We find no particular advantage to either design in this comparison, but both configurations can be improved, as we will see later.



Figure 4.1. IRA-1 with feed arms at  $\pm 45^\circ$ .



Figure 4.2. IRA-2 with feed arms at  $\pm 30^\circ$ .

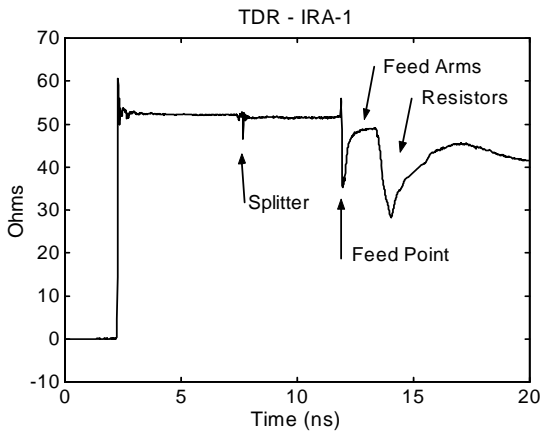


Figure 4.3. TDR of the IRA-1.

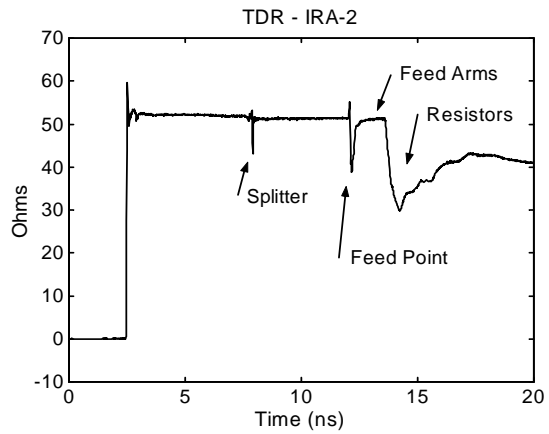


Figure 4.4. TDR of the IRA-2.

Next, we compare the TDRs of the two Collapsible IRAs (CIRAs) as described in [1]. The CIRA-1 and CIRA-2 are shown in Figures 4.5 and 4.6, respectively. These antennas have a diameter of 1.22 m (48 in.) with a focal length of 49 cm ( $F/D = 0.4$ ). The CIRA-1 has feed arms positioned at  $\pm 45^\circ$  to vertical and the CIRA-2 has feed arms positioned at  $\pm 30^\circ$  to vertical. The reflector and feed arms for the collapsible antennas are made from nylon fabric that is plated with nickel over copper (CIRA-1) or nickel over silver (CIRA-2).

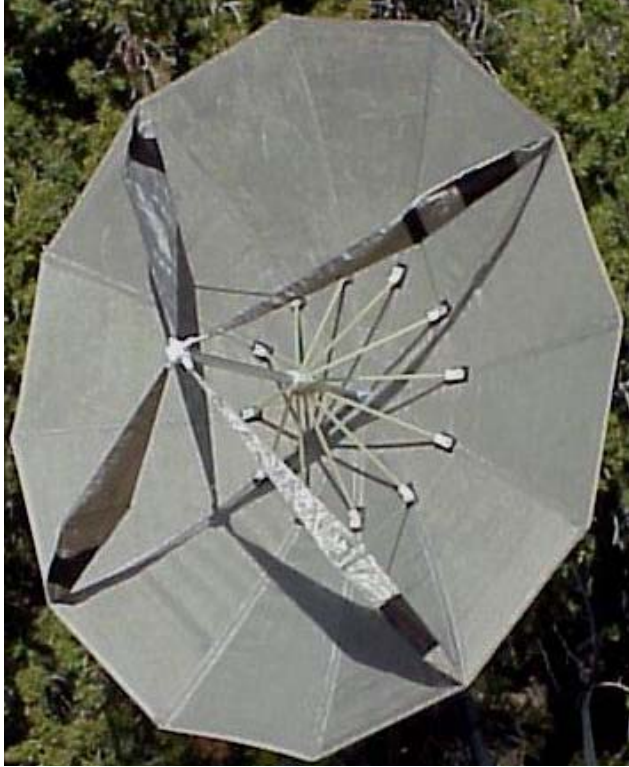


Figure 4.5. CIRA-1 with feed arms at  $\pm 45^\circ$ .



Figure 4.6. CIRA-2 with feed arms at  $\pm 30^\circ$ .

The load resistance at the end of the feed arms is made from a woven polyester fabric treated with polypyrrole, which has a resistance of approximately  $185 \Omega/\text{square}$ . The resistive fabric provides a highly distributed load at the ends of the feed arms. The feed arms on the CIRA-1 have a reverse taper beginning at a distance  $F$  from the feed point as did the IRA-1 and IRA-2. However, the CIRA-2 has the load resistance starting at a distance  $F$  from the feed point. The resistive fabric is the dark area between the end of each feed arm and the reflector. The resistance of these fabric sections is close to  $200 \Omega$ .

The TDRs of the CIRA-1 and CIRA-2 are shown in Figures 4.7 and 4.8. The TDR of the CIRA-1 is quite smooth at the resistors, while that of the CIRA-2 has a small bump. This comparison tends to argue in favor of positioning feed arms at  $\pm 45^\circ$ , but the advantage is small. We will see later that optimal performance in  $\pm 30^\circ$  designs is obtained when the resistors are concentrated at the edge of the feed arms, instead of being evenly distributed. However, a configuration with the resistance concentrated at the edges is challenging to manufacture in a fabric resistor. We discuss the position of resistors in further detail in Section VIII of this paper.

The TDRs in the two CIRAs are generally better (flatter) at the resistors than those of the IRA-1 and IRA-2 shown previously. We hypothesized that this was due to the distributed nature of the resistive load. This led us to try modifying the resistors in the IRA-1 and IRA-2 to make them more distributed. We examine this case next.

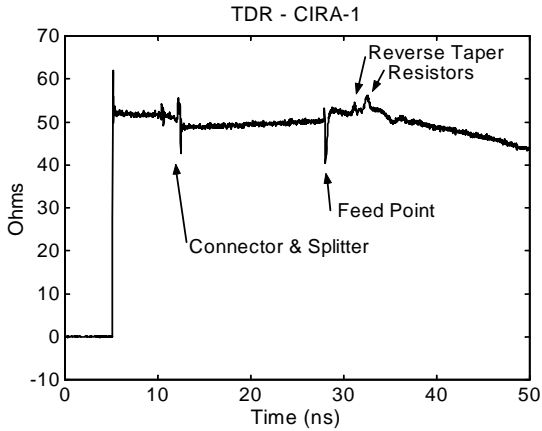


Figure 4.7. TDR of the CIRA-1.

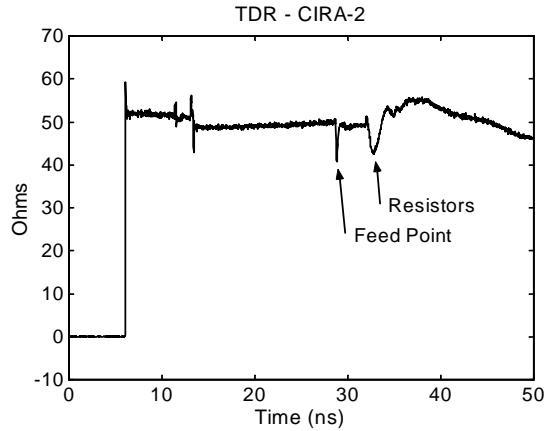


Figure 4.8. TDR of the CIRA-2.

Next, we modified versions of the IRA-1 and IRA-2 to use distributed resistors. The two modified antennas, called the IRA-1B and IRA-2B, are shown in Figures 4.9 and 4.10. In both cases the distributed resistance is made up of five strings of resistors in parallel. Each string is made up of three resistors in series totaling  $1000\ \Omega$ . The resistors used for this experiment were  $\frac{1}{2}$ -Watt metal film resistors.

The TDRs of the IRA-1B and IRA-2B with distributed loads are shown in Figures 4.11 and 4.12. The horizontal line on the plots at  $40\ \Omega$  helps show that the mismatch at the load is slightly less on the IRA-1B than the IRA-2B. This might suggest that the configuration with feed arms at  $\pm 45^\circ$  is preferred. However, further improvement can be made in the  $\pm 30^\circ$  design by concentrating the resistance at the edge of the feed arms, as we shown in the next case.



Figure 4.9. IRA-1B with distributed load.

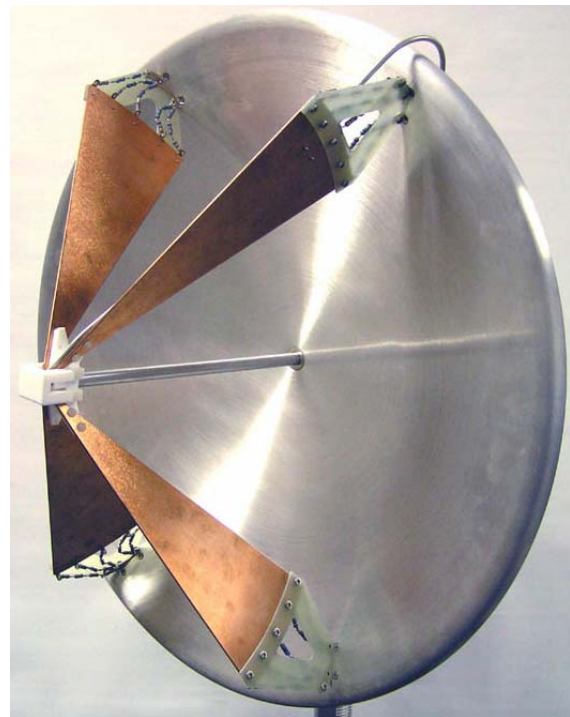


Figure 4.10. IRA-2B with distributed load.



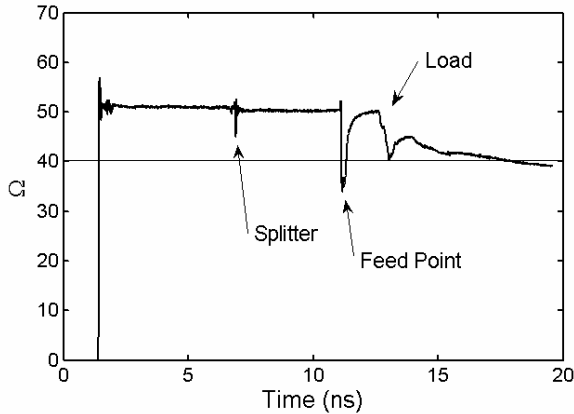


Figure 4.11. TDR of the IRA-1B with distributed load.

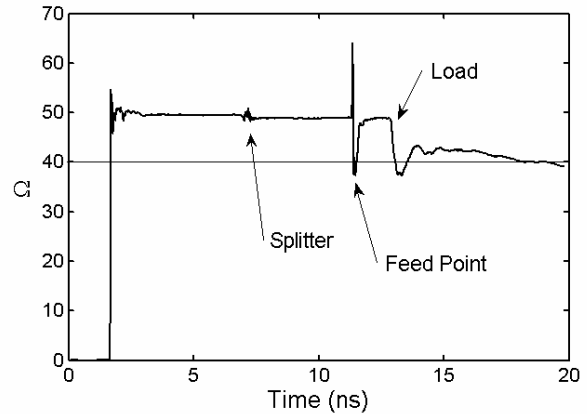


Figure 4.12. TDR of the IRA-2B with distributed load.

Until now, the best configuration in an IRA with solid reflector has been the IRA-1B ( $\pm 45^\circ$ ) with distributed resistors. After much experimentation, we found we could improve the  $\pm 30^\circ$  design by arranging the resistors into two strings positioned near the edge of the feed arms. To test this, we compare the TDR of the IRA-3 to that of the IRA-1B with distributed resistors.

The IRA-3, shown in Figure 4.13, has the feed arms positioned at  $\pm 30^\circ$  to vertical, as with the IRA-2, and it also has a ground plane located on the horizontal plane of symmetry. The ground plane has no effect on the TDR comparison. We performed numerous experiments on the IRA-3 to improve the TDR at the load. These experiments are described in some detail in [2]. We found the best TDR is obtained by using two resistor strings connected to the corners of the feed arms, as shown in Figure 4.14. Note that the corners of the feed arms are trimmed so that the load begins slightly before the distance  $F$  from the feed point.

The TDR of the IRA-3 is shown in Figure 4.15. For convenience, in this figure we have also reproduced the TDR of the IRA-1B with distributed load from Figure 4.11. Comparing these two TDRs, we find them to be quite similar. There is perhaps a small advantage to the IRA-1B with distributed load ( $\pm 45^\circ$ ), but this difference is negligible.



Figure 4.13. IRA-3.

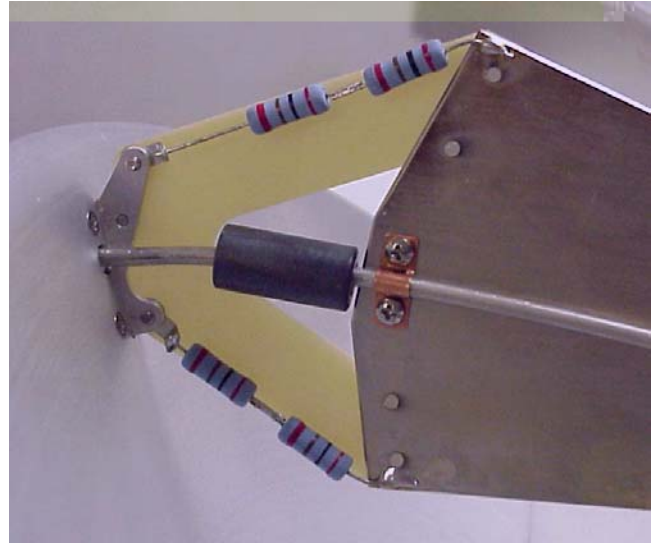


Figure 4.14. IRA-3 load with two resistor strings.

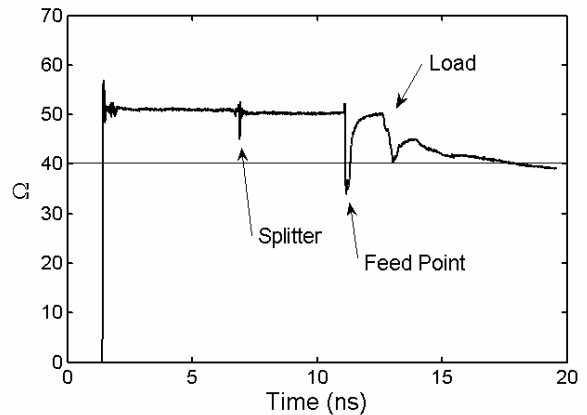
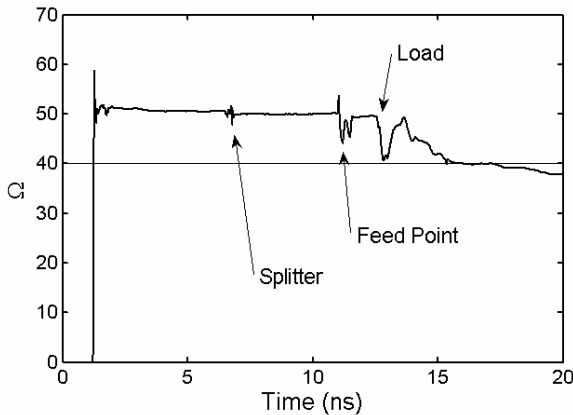


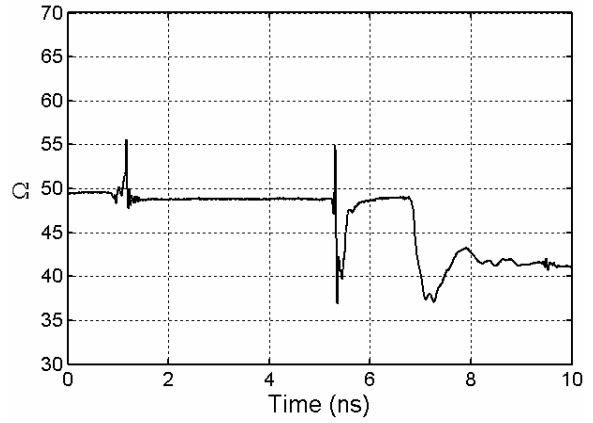
Figure 4.15. TDR of the IRA-3 (left) and IRA-1B with distributed load (right).

## V. The Effect of Cable Position

One theory about why the TDRs in [4,5] and Section II are so flat is that the chokes are not effective in suppressing the exterior cable current over the entire frequency range of interest. If this were true, then positioning the feed cable a significant distance away from the resistors, as in [4,5], might help to reduce the tendency of the cable to short out the resistors. We tested that theory by modifying our IRA-2B so the cable runs as far as possible away from the resistors. We compare two configurations in Figure 5.1. On the top of this figure are photos and the TDR of the IRA-2B with the normal cable placement. On the bottom are the photos and TDR of the same configuration with the cable displaced to avoid the resistors. We observe very little difference in the TDRs, so we tentatively conclude that cable position is not critical.



Cable in Normal Position,  
Close to Resistors



Cable in Displaced Position,  
Away from Resistors

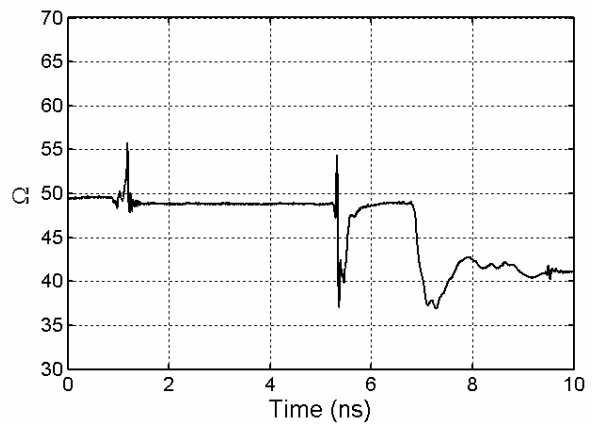


Figure 5.1. IRA-2B with distributed resistors. The cable is in the normal position (top) and in a displaced position (bottom). Also shown are the TDRs of the two configurations.

## VI. Carbon-Composition vs. Metal-Film Resistors

Next, we tested the effect of replacing the metal-film resistors in the IRA-2B with small  $\frac{1}{2}$ -Watt carbon-composition resistors manufactured by Ohmite. This modified IRA-2 is called the IRA-2C. The resistor configuration of the IRA-2B and IRA-2C are shown in Figure 6.1, and the resulting TDRs are shown in Figure 6.2. We observe no appreciable difference between the two, suggesting that carbon-composition resistors make little difference.



Figure 6.1. Resistor configuration of the IRA-2B, with metal-film resistors (left) and the IRA-2C, with carbon-composition resistors (right).

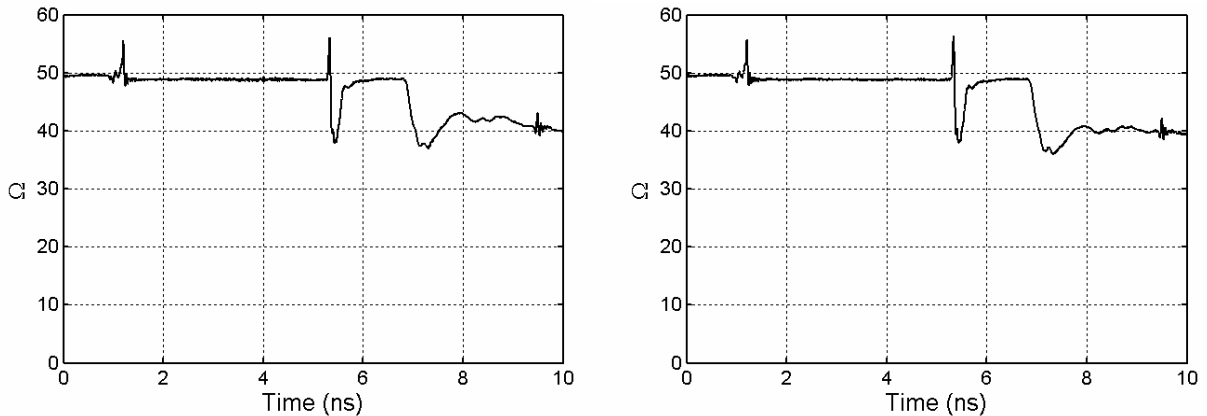


Figure 6.2. TDRs of the IRA-2B, left and the IRA-2C, right.

## VII. A Second Example of a Large IRA with Smooth TDR

In order to determine the effect of using metal-film resistors in large IRAs, we built a large IRA with a diameter of 1.52 m (5-ft.). This device, called the IRA-6, had feed arms positioned at  $\pm 45^\circ$  to vertical and included a ground plane, as shown in Figure 7.1. We designed the IRA-6 to tolerate voltages as high as 30 kV for pulse widths less than 5 ns, so the antenna included a custom high-voltage splitter balun. This balun used a custom cable that is roughly equivalent to RG-213 in diameter, with a narrower center conductor to realize a 100- $\Omega$  impedance. We used an HN-Type connector at the input port, and we had bare cable stubs at the feed point 19 mm (0.75 in.) in length to protect against flashover. A close-up of the feed point is shown in Figure 7.2. The resistive load consisted of seven strings of 2-Watt metal film resistors, as shown in Figure 7.3. The material supporting the resistors at the end of the feed arms is Lexan polycarbonate with a thickness of 5 mm (3/16 in.) that has been drilled with many holes.



Figure 7.1 The IRA-6.

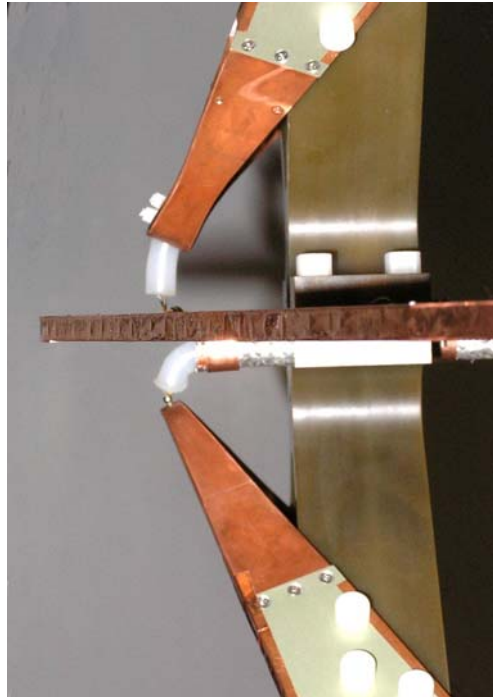


Figure 7.2. Feed point of the IRA-6.

The TDR of the IRA-6 is shown in Figure 7.4, and we note a number of features. First, it is remarkably smooth at the resistors, even though we used metal-film (not carbon-composition) resistors. There is a significant bump at the feed point, despite many attempts to smooth it out. We believe the bump is probably inevitable because of the 19-mm cable stubs at the feed point.

The data provided here is of interest because it suggests that it is relatively easier to obtain a smooth TDR in large IRAs than in smaller ones. We used metal-film resistors—not the carbon composition ones that are normally thought to have lower inductance. We suspect that the size of the antenna introduces losses into the cable and feed arms that mask the reflections back from the load. Further detail on this antenna, including pattern data, will be published in a future note.

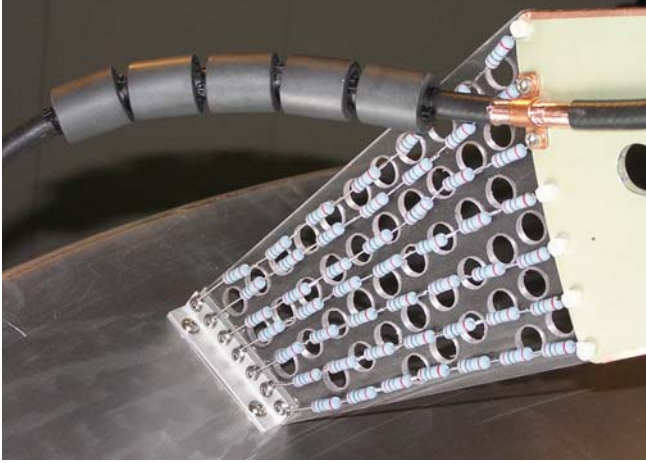


Figure 7.3. Resistive load of the IRA-6.

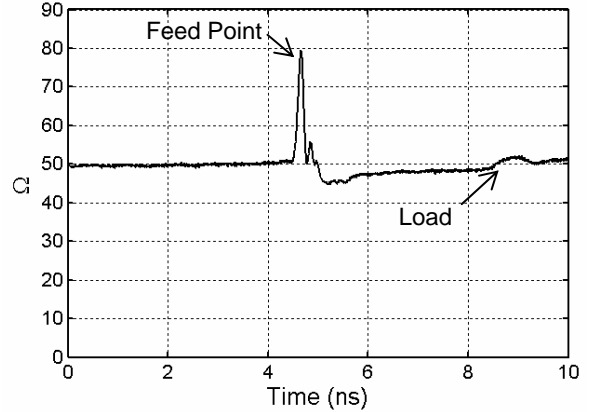


Figure 7.4. TDR of the IRA-6.

### VIII. The Effect of Resistor Position

Finally, we consider the effect of the resistor position with respect to the edge of the feed arms. It has been noted by some that this can affect the smoothness of the TDR. When terminating flat-plate EMP simulators, it has become customary to space the resistors so an equal current goes through each one [6]. This is normally implemented by adding a sawtooth pattern to the end of the flat plate, with wide teeth in the center and narrow teeth at the edge.

The current distribution on a flat plate is approximated by [6]

$$J_s(x) = \frac{J_o}{\pi \sqrt{1 - (x/a)^2}} \quad (8.1)$$

where  $a$  is the half-width of the plate,  $J_o a$  is the total current on the plate, and  $x$  is the distance from the center line. The current along a given segment is the integral of this distribution over a segment, or

$$I_n = \int_{x_{n-1}}^{x_n} J_s(x) dx = J_o \frac{a}{\pi} \left[ \arcsin\left(\frac{x_n}{a}\right) - \arcsin\left(\frac{x_{n-1}}{a}\right) \right] \quad (8.2)$$

where  $x_n$  is the edge of the  $n^{\text{th}}$  segment. Additional details are provided in [6].

The large antennas described in [4,5] used several resistor strings in an attempt to approximate the above distribution, as seen in Figure 2.2 of this paper. In smaller antennas, it is much more challenging to place large numbers of resistor strings in precise positions. This may be one reason why the larger antennas tend to have flatter TDRs at their terminations.

## IX. Discussion

The large antennas described in [4, 5] and in Section II of this paper had the best TDRs, and they had feed arms positioned at  $\pm 45^\circ$ . But this provides insufficient information to infer the superiority of the  $\pm 45^\circ$  design because of their other properties. First, they had no splitter baluns, which may have made it easier to establish a smooth impedance match. Second, there was no attempt to compare two different feed arm positions in similar IRAs; the authors simply looked at IRAs with feed arms positioned at  $\pm 45^\circ$ . Without a control configuration, it is difficult to draw a firm conclusion about the relative advantages of the two feed arm positions. Third, the antennas were larger, which might introduce losses into the longer lengths of cable. These losses may have obscured reflections from the resistors. The larger size also allows more precise positioning of the resistors. Finally, the cable was arranged to avoid the resistors, which also might be expected to help, although we did not observe that effect in Section V of this paper.

We experimented with two different kinds of carbon-composition resistors, as shown in Figures 4.1, 4.2, and 6.1. We found no advantage in either of these two resistor types over the metal-film resistors that we typically use. We also built and tested a large IRA with feed arms at  $\pm 45^\circ$  using metal-film resistors. We observed a very smooth TDR at the loads, which suggests that carbon-composition resistors may not be necessary for proper impedance matching.

Since the best TDR performance was obtained with a large IRA with feed arms at  $\pm 45^\circ$ , the issue of the optimal position of the feed arms remains unresolved. This will be resolved only when similar performance is demonstrated in a large IRA with feed arms at  $\pm 30^\circ$ . Nevertheless, we have compelling evidence that we expect that will be the case, based on our data with smaller IRAs.

## X. Conclusions

By comparing the TDRs of similar IRAs, we have attempted to answer the question of the optimal feed arm position in reflector IRAs. The challenge has always been that small IRAs with feed arms at  $\pm 30^\circ$  seem not to have as flat a TDR as large IRAs with feed arms at  $\pm 45^\circ$ . But this has been a comparison in which a large number of variables were not controlled. These variables include the reflector size, the resistor type (metal film or carbon composition), the resistor size, and whether or not a balun was used.

In cases where all the variables are controlled, we have shown that designs with feed arms at  $\pm 30^\circ$  are preferred, because there is a negligible penalty in TDR, and a significant advantage in copol and crosspol realized gain. The comparison in Figure 4.15 should be persuasive.

The question will never be fully resolved until a controlled comparison is made between two large IRAs with carbon composition resistors. Other variables that should be controlled include the presence or absence of a splitter balun and ground plane. We have provided compelling evidence that that this experiment is worth trying, in order to verify the improved performance of  $\pm 30^\circ$  designs observed in smaller IRAs.

## Acknowledgement

We wish to thank the Air Force Research Laboratory, Directed Energy Directorate, for funding this work. We also wish to thank Dr. David V. Giri for helpful discussions on this work, and for providing the data from Reference [5] that was reproduced in Section II of this paper. Finally, we wish to thank Dr. Carl E. Baum for helpful discussions on this work.

## References

1. L. H. Bowen, E. G. Farr, C. E. Baum, T. C. Tran, and W. D. Prather, "Experimental Results of Optimizing the Location of Feed Arms in a Collapsible IRA and a Solid IRA," Sensor and Simulation Note 450, November 2000.
2. L. H. Bowen, E. G. Farr, C. E. Baum, T. C. Tran, and W. D. Prather, "Results of Optimization Experiments on a Solid Reflector IRA," Sensor and Simulation Note 463, January 2002.
3. J. S. Tyo, "Optimization of the TEM Feed Structure for Four-Arm Reflector Impulse Radiating Antennas, *IEEE Trans. Antennas and Propagat.* Vol. 49, No. 4, April 2001, pp. 607-614. This also appeared as "Optimization of the Feed Impedance for an Arbitrary Crossed-Feed-Arm Impulse Radiating Antenna," Sensor and Simulation Note 438, November 1999.
4. D. V. Giri, H. Lackner, *et al*, A Reflector Antenna for Radiating Impulse-Like Waves, Sensor and Simulation Note 382, July 1995. The TDR data also appeared in D. V. Giri and H. Lackner, Preliminary Evaluation of the Terminating Impedance in the Conical-Line Feed or IRAs, Prototype IRA Memo 2, May 1994.
5. M. Abdalla, M. Skipper, D. V. Giri, *et al*, Evaluation of the Terminating Impedance in the Conical-Line Feed of the 6-foot IRA, Prototype IRA Memo 8, April 2001.
6. D. V. Giri and C. E. Baum, Design Guidelines for Flat-Plate Conical Guided-Wave EMP Simulators with Distributed Terminations, Sensor and Simulation Note 402, October 1996.